ARTICLE

Cystathionine-γ-lyase ameliorates the histone demethylase JMJD3-mediated autoimmune response in rheumatoid arthritis

Weijun Wu[1,2], Ming Qin[1], Wanwan Jia[1], Zheng Huang[3], Zhongzheng Li[4], Di Yang[1], Mengwei Huang[1], Chenxi Xiao[1], Fen Long[1], Jianchun Mao[5], Philip K. Moore[6], Xinhua Liu[1] and Yi Zhun Zhu[1,2]

Cystathionine-γ-lyase (CSE), an enzyme associated with hydrogen sulfide (H_2S) production, is an important endogenous regulator of inflammation. Jumonji domain-containing protein 3 (JMJD3) is implicated in the immune response and inflammation. Here, we investigated the potential contribution of JMJD3 to endogenous CSE-mediated inflammation in rheumatoid arthritis (RA). Upregulated CSE and JMJD3 were identified in synovial fibroblasts (SFs) from RA patients as well as in the joints of arthritic mice. Knocking down CSE augmented inflammation in IL-1β-induced SFs by increasing JMJD3 expression. In addition, $CSE^{-/-}$ mice with collagen-induced arthritis (CIA) developed severe joint inflammation and bone erosion. Conversely, overexpressing CSE inhibited JMJD3 expression by the transcription factor Sp-1 and was accompanied by reduced inflammation in IL-1β-treated SFs. Furthermore, JMJD3 silencing or the administration of the JMJD3 inhibitor GSK-J4 significantly decreased the inflammatory response in IL-1β-treated SFs, mainly by controlling the methylation status of H3K27me3 at the promoter of its target genes. GSK-J4 markedly attenuated the severity of arthritis in CIA mice. In conclusion, suppressing JMJD3 expression by the transcription factor Sp-1 is likely responsible for the ability of CSE to negatively modulate the inflammatory response and reduce the progression of RA.

Keywords: cystathionine-γ-lyase; rheumatoid arthritis; Jumonji domain-containing protein 3; Sp-1; Toll like receptor 2

Cellular & Molecular Immunology (2019) 16:694–705; https://doi.org/10.1038/s41423-018-0037-8

INTRODUCTION

Rheumatoid arthritis (RA) is an autoimmune disease involving inflammation of the synovium in peripheral joints, progressing to the destruction of articular cartilage, triggering joint degeneration, pain and loss of function.[1–4] Early intensive treatment, including the addition of a biological agent, is recommended for patients with RA, but up to 50% patients with RA fail to respond adequately.[5,6] In addition, biologics and other anti-rheumatic drugs may be associated with long-term side effects,[7] including serious infections and malignancies.[8] Thus, there are clear unmet demands to develop more effective and safer therapeutic approaches for RA.

There is considerable evidence suggesting that epigenetic mechanisms mediate the development of inflammation by modulating the expression of inflammatory cytokines.[9,10] Jumonji domain-containing protein 3 (JMJD3; also known as KDM6B) is induced by inflammatory stimuli.[11] JMJD3 specifically demethylates trimethylated lysine 27 in histone H3 (H3K27me3), a chromatin modification associated with transcriptional repression.[12] The role of JMJD3 in RA may lie at the intersection of many pathways promoted in a dysfunctional manner.

Hydrogen sulfide (H_2S) belongs to the class of endogenous gases that include nitric oxide and carbon monoxide (CO) and plays an important role in regulating inflammatory responses.[13] H_2S is produced physiologically by the action of the pyridoxal-5′-phosphate-dependent enzymes cystathionine-γ-lyase (CSE) and cystathionine-β-synthase (CBS).[14] CBS is abundantly expressed in the brain, while CSE shows higher expression in the liver, kidney and peripheral tissue.[15,16] The exact mechanisms of the actions of H_2S, as an inflammatory mediator, are not well established; however, existing data indicate multiple, diverse targets.[17–19] In our recent study, we found that CSE/H_2S modulates inflammation in RA,[20] but whether H2S regulates inflammation by affecting histone methylation modification has not been reported.

Given the role of JMJD3 and CSE/H_2S in various inflammatory diseases, further work is needed to identify potential points for 'crosstalk' between JMJD3 and CSE/H_2S in RA. We hypothesize that JMJD3 may be involved in the anti-inflammatory effect of CSE/H_2S in RA. The present results show, for the first time, that endogenous CSE produces powerful anti-inflammatory effects by regulating the transcription factor Sp-1 to inhibit JMJD3 expression in RA. This conclusion was additionally confirmed in synovial fibroblasts (SFs) from human RA samples.

[1]Department of Pharmacology, Shanghai Key Laboratory of Bioactive Small Molecules, School of Pharmacy, Fudan University, Shanghai 201203, China; [2]State Key Laboratory of Quality Research in Chinese Medicine and School of Pharmacy, Macau University of Science and Technology, Macau, China; [3]Institute of Arthritis Research, Shanghai Academy of Chinese Medical Sciences, Guanghua Integrative Medicine Hospital/Shanghai University of T.C.M, Shanghai, China; [4]Ningbo The 9th Hospital, Ningbo 315000, China; [5]Department of Rheumatology, Shanghai Longhua Hospital, Shanghai, China and [6]Department of Pharmacology, National University of Singapore, Singapore, Singapore
Correspondence: Xinhua Liu (liuxinhua@fudan.edu.cn) or Yi Zhun Zhu (yzzhu@must.edu.mo)

Received: 6 November 2017 Revised: 15 April 2018 Accepted: 22 April 2018
Published online: 29 May 2018

MATERIALS AND METHODS

Materials

Recombinant human interleukin (IL)-1β was purchased from Peprotech (Rocky Hill, NJ, USA). Chick type II collagen (CII) and Freund adjuvant (CFA) were obtained from Chondrex (CII; Chondrex, Redmond, WA, USA). The JMJD3 inhibitor GSK-J4 was purchased from Selleck Chemicals LLC (Houston, TX, USA). Macrophage colony-stimulating factor (M-CSF), receptor activator of nuclear factor (NF)-κB ligand (RANKL) and H_2S inhibitor DL-propargylglycine (PAG) were purchased from Sigma-Aldrich (St. Louis, MO, USA). Mithramycin (Sp-1 inhibitor), BIRB769 (p38 inhibitor) and U0126 (ERK inhibitor) were purchased from Calbiochem (San Diego, CA). The antibodies were obtained from the following commercial sources: JMJD3 was purchased from Novus (Novus Biologicals, USA); phosphor (p)-ERK1/2 (Thr^{202}/Tyr^{204}), ERK1/2, p-JNK (Thr^{183}/Tyr^{185}), JNK, p-p38, p38, Sp-1, IL-6, COX-2 and H3K27me3 were purchased from Cell Signaling Technology (Beverly, MA); p-Sp-1 (Thr^{739}) was purchased from GeneTex (GeneTex Inc. USA); and CSE, TLR2 and glyceraldehyde-3-phosphate dehydrogenase (GAPDH) were obtained from Santa Cruz Biotechnology (Santa Cruz, CA, USA).

Ethics statements

All experimental protocols using animals conformed to the Animal Welfare Act Guide for Use and Care of Laboratory Animals and were approved by the Institutional Animal Care and Use Committee, School of Pharmacy, Fudan University, China.

Induction of CIA and treatment

Male DBA/1J mice, aged 6–8 weeks, were purchased from Shanghai SLAC Laboratory Animal Co. Ltd, Shanghai, China. The CSE knockout C57BL/6 mice were a gift from the Shanghai Research Center of Model Organisms, Shanghai, China. The CSE knockout mice on a DBA/1J background ($CSE^{-/-}$) were generated by crossing the CSE knockout mice with the DBA/1J mice, and the littermate mice were used as wild type (WT). The induction of collagen-induced arthritis (CIA) was performed as described in a previous study.[21] The WT and $CSE^{-/-}$ mice were killed on day 30 after the second immunization.

Male DBA/1J mice were used to evaluate the anti-arthritic effect of GSK-J4 in vivo. The GSK-J4 treatment group was given a daily intraperitoneal injection of GSK-J4 (20 mg/kg of body weight, $n = 8$) until the end of the experiment on day 40 after the second immunization. GSK-J4 was dissolved in dimethyl sulfoxide and was then diluted with phosphate-buffered saline to the final concentration.

Isolation and culture of human SFs

Human synovial samples were obtained from the knee joints of 6 patients with RA treated in the Guanghua Integrative Medicine Hospital, Shanghai, China. Control synovial samples from 6 healthy donors and 6 patients with osteoarthritis (OA) were obtained from Ningbo The 9th Hospital, Ningbo, China. All of the patient samples were taken with patient consent and full local regional ethics committee. The SFs were obtained by enzymatic digestion as previously described.[22] The cells were grown in Dulbecco's modified Eagle's Medium with 10% fetal bovine serum (FBS; Gibco BRL, Frederick, MD, USA). The SFs were cultured for six to eight passages, and the lysate was then collected for the analyses.

Bone mineral density measurement

The left femur of each mouse was fixed and the whole femur was scanned by a high speed in vivo μCT scanner (Quantum FX, PerkinElmer, MA, USA). Three-dimensional images were reconstructed in the region of interest, and the bone mineral density (BMD; mg/cm^3) was assessed using the micro-computed tomography (CT) software.[23]

Histological and immunohistochemical analysis of the joint tissue

For the histologic analysis, the paws were fixed in 4% buffered formaldehyde, decalcified in ethylene diaminetetraacetic acid, embedded in paraffin and cut into 4 μm sections, which were then stained with hematoxylin and eosin (H&E). Additional sections were stained with safranin O or toluidine blue to evaluate cartilage damage. An immunohistochemical analysis was performed on the deparaffinized tissues. The samples were subjected to antigen retrieval by boiling in 10 mM citrate buffer (pH 6.0) for 10 min, treated with 1% H_2O_2 for 10 min, and blocked with 5% bovine serum albumin (BSA) for 1 h at room temperature. The tissue sections were then further incubated with primary antibodies overnight. After incubation with anti-rabbit horseradish peroxidase (HRP)-conjugated secondary antibody for 90 min, the sections were visualized by 3,3′-diaminobenzidine-tetrahydrochloride (DAB). The stained tissue sections were imaged using an Axio Scope.A1 microscope (Zeiss) at the indicated magnification.

Cell culture and treatment

The fibroblast-like synoviocyte MH7A cell line was a gift from Professor Zhang Peng (Chinese Academy of Science, Shenzhen). The MH7A cells were cultured in Roswell Park Memorial Institute 1640 medium (HyClone), supplemented with 10% FBS and 1% penicillin/streptomycin in a 5% CO_2 humidified atmosphere at 37 °C. The cells were stimulated with IL-1β (10 ng/ml), and all of the inhibitors were administered for 1 h prior to cytokine stimulation.

Small interfering RNA (siRNA) transfection

The JMJD3 siRNA (5′-GCGAUGUGUGGAGGUGUUUAATT-3′) and control siRNA (5′-CGUUAAUCGCGUAUAAUACGCGUAT-3′) were produced by GenePharma (Shanghai, China). To introduce the siRNA into the cells, the cells were plated on 6-well plates at 30% to 50% confluence before transfection. The siRNA transfection was carried using Lipofectamine RNAiMAX following the manufacturer's instructions.

Lentivirus generation and infection

The specific short hairpin RNA (shRNA) Sp-1 and the Sp-1-cDNA plasmids were gifts from Professor Zeng (State Key Laboratory of Oncology in South China, Sun Yat-sen University Cancer Center, Guangdong) and Professor Wu (Department of Biochemistry and Molecular Biology, Shanghai Medical College, Fudan University, Shanghai), respectively. The shRNA CSE, CSE-cDNA and shRNA-control (Ctl) plasmids were kind gifts from Professor Zha (Department of Biochemistry and Molecular Biology, Fudan University, Shanghai). Lentivirus generation and infection were performed according to the procedure described previously.[20]

Quantitative real-time reverse transcription-polymerase chain reaction (qRT-PCR) analysis

Total RNA was isolated with the TRIzol Reagent (Invitrogen, Carlsbad, CA, USA) following the manufacturer's instructions. Total RNA (2 μg) was reverse-transcribed into complementary DNA (cDNA) using a two-step RT Kit (Takara Biotechnology, Dalian, China) according to the manufacturer's directions. See Table S1 for the primer sequences.

Western blot analysis

An equal amount of protein from each cell lysate was resolved on an SDS-polyacrylamide gel and was transferred to a nitrocellulose membrane. Nonspecific binding was blocked by incubating the blots with 5% nonfat dry milk powder in TBST (20 mM Tris-HCl (pH 7.4), 137 mM NaCl, and 0.1% Tween 20) for 60 min. The blots were incubated overnight at 4 °C with primary antibody followed by an incubation with an anti-rabbit-HRP or anti-mouse-HRP secondary antibody in 5% BSA for 2 h. After washing in TBST, the immunoblots were developed with an enhanced

chemiluminescence detection system (Millipore) as per the manufacturer's instructions. GAPDH was used as a loading control.

Cytokine measurement
The cytokine levels were determined by enzyme-linked immunosorbent assay (ELISA) kits (Boatman Biotechnology, Shanghai, China) according to the manufacturer's instructions. The optical densities were read on a microplate reader (M1000, TECAN, Austria GmbH, Austria) at 450 nm.

Chromatin immunoprecipitation
The assay for chromatin immune-precipitation (ChIP) was performed using the EZ-ChIP™ Chromatin immune-precipitation kit (Millipore) according to the manufacturer's instructions. The DNA pulled down by the anti-MYC or H3K27me3 antibodies was amplified by PCR. The DNA from these samples was subjected to PCR analyses with primers sets for the JMJD3 (KDM6B) or TLR2 promoter.

Electrophoretic mobility shift assays (EMSA)
Nuclear protein was extracted with a nuclear protein extraction kit (Invitrogen) in accordance with the manufacturer's instructions. The biotinylated Sp-1 oligonucleotide probe was 5′-GGGCTGGGGGGGCGGGTAGTTAAAG-3′, and the mutant probe was 5′- ATTCGATCGGTTCGGGGCGAGC -3′. The binding reactions were performed according to the non-radioactive EMSA kit. The specificity of the DNA and protein complex was confirmed by cold competition with a 50-fold excess of unlabeled Sp-1 oligonucleotides. After the binding reaction, gel electrophoresis, membrane transfer and immobilization, a chemiluminescent reaction and imaging were performed sequentially.

Immunofluorescence analysis
For the immunofluorescence analysis, the cells were immunostained using primary antibodies overnight, and the secondary antibodies used were Alexa Fluor 488 donkey anti-rabbit or mouse IgG (1:200 dilution, Thermo Fisher Scientific). The nuclei were stained with 6-diamidino-2-phenylindole (DAPI). The sections were observed by confocal laser scanning microscopy (Zeiss LSM780, Carl Zeiss).

Osteoclastogenic differentiation
Osteoclasts were differentiated from mouse bone marrow monocytes (BMMs) as previously described.[24] Briefly, the BMMs were cultured with 40 ng/ml of M-CSF in α-Minimum Essential Medium containing 10% FBS for 3 days until the cells reached confluence. The cells were then differentiated with M-CSF (40 ng/ml) and RANKL (50 ng/ml) in the presence of PAG or GSK-J4. At day 6, the cells were fixed with 2.5% glutaraldehyde (Sigma). The osteoclasts were identified by the tartrate-resistant acid phosphatase (TRAP) staining kit (Sigma/Aldrich). Mature osteoclasts were identified as multinucleated (>3 nuclei) $TRAP^+$ cells. Cell images were obtained using a Zeiss microscope.

Cell viability assay
BMMs were seeded in 96-well plates at a density of 1.25×10^4 cells/well. The cells were treated with GSK-J4 (0.5, 1, 5, 10, 20 μM) or PAG (0.5, 1, 2, 4, 8 mM) for 48 h. A cell viability assay was performed by using CCK8 cell count Kit (Dojindo Laboratories, Japan) according to the manufacturer's protocol. All of the values were standardized by comparison with the data from the untreated cells.

Migration assay
Following the transfection with the siRNA for JMJD3, the CSE-specific shRNA or the control shRNA for 48 h, the MH7A cells were subjected to a migration assay, which was performed with a transwell chamber with an 8 μm pore (Corning, USA) according to our previously described method.[20] The migrated cells were stained with crystal violet.

Statistical analysis
The statistical analysis was performed using GraphPad Prism version 5.0. All of the values are expressed as the mean ± SEM. A one-way analysis of variance was initially performed to determine whether an overall statistically significant change existed before using the two-tailed paired or unpaired Student's *t*-test. A value of $p < 0.05$ was considered statistically significant.

RESULTS

Establishing an inflammatory response in IL-1β-induced MH7A cells
IL-1β is a pivotal inflammatory cytokine that is known to induce the generation of a range of additional inflammatory cytokines.[25] As illustrated in Fig. S1, IL-1β (10 ng/ml) dramatically increased IL-6, IL-23 and matrix metallopeptidase 9 (MMP9) messenger RNA (mRNA) expression in MH7A cells. Similarly, the mRNA and protein levels of cyclooxygenase-2 (COX-2) and tumor necrosis factor-α (TNF-α) in the IL-1β-stimulated MH7A cells were also significantly increased. Toll-Like receptor 2 (TLR2) might contribute to sustaining inflammation, and our results also exhibited that the mRNA and protein expression levels of TLR2 were markedly increased with IL-1β stimulation. Taken together, these results suggested that IL-1β-stimulated MH7A cells displayed a heightened inflammatory response state, as illustrated by the increased pro-inflammatory mediators.

CSE negatively regulates the inflammatory response in IL-1β-induced MH7A cells
CSE is the primary enzyme responsible for the generation of H_2S in peripheral tissues. As illustrated in Fig. 1a, IL-1β time-dependently increased CSE protein expression in MH7A cells. Transfection with lentivirus vectors expressing CSE (LV-CSE) resulted in the overexpression of CSE in the MH7A cells and caused a reduction in the COX-2 and IL-6 mRNA levels compared to the cells transfected with the vector controls (LV-Ctl) (Fig. 1b). Furthermore, the overexpression of CSE inhibited COX-2 protein expression as well as TNF-α and IL-6 secretion in the supernatants of the IL-1β-stimulated MH7A cells (Fig. 1c, d). In contrast, CSE-shRNA transfection resulted in a decrease in CSE expression but an increase in COX-2 and IL-6 expression (Fig. 1e, f). Meanwhile, the knockdown of CSE markedly increased TNF-α and IL-6 generation in the MH7A cells (Fig. 1g). Taken together, these findings strongly suggest that CSE negatively regulates the inflammatory response in IL-1β-stimulated MH7A cells.

JMJD3 inhibition represses the inflammatory response partly by mediating TLR2 expression in IL-1β-induced MH7A cells
The mRNA and protein expression levels of JMJD3 in the MH7A cells exposed to IL-1β rapidly increased (Fig. 2a). Membrane receptors are universally recognized as important mediators of the inflammatory response. Thus, we carried out a heatmap analysis of membrane receptors using the SFs from RA patients. A hierarchical clustered heatmap analysis showed that TLR2 exhibited a maximum relative abundance in the RA-SF groups at the transcriptional level (Fig. 2b; note that the green and red represent the minimal and the maximal relative abundance, respectively). As such, we hypothesized that IL-1β regulated JMJD3 expression to affect TLR2 transcription. To explore this possibility, we silenced JMJD3 expression and found that the knockdown of JMJD3 inhibited TLR2 mRNA expression in response to IL-1β (Fig. 2c), and that it also inhibited TLR2 and COX-2 protein expression (Fig. 2d). We next used the JMJD3 inhibitor GSK-J4.[26] As expected, GSK-J4 concentration-dependently attenuated the upregulation of TLR2 and COX-2 induced by IL-1β (Fig. 2d). The

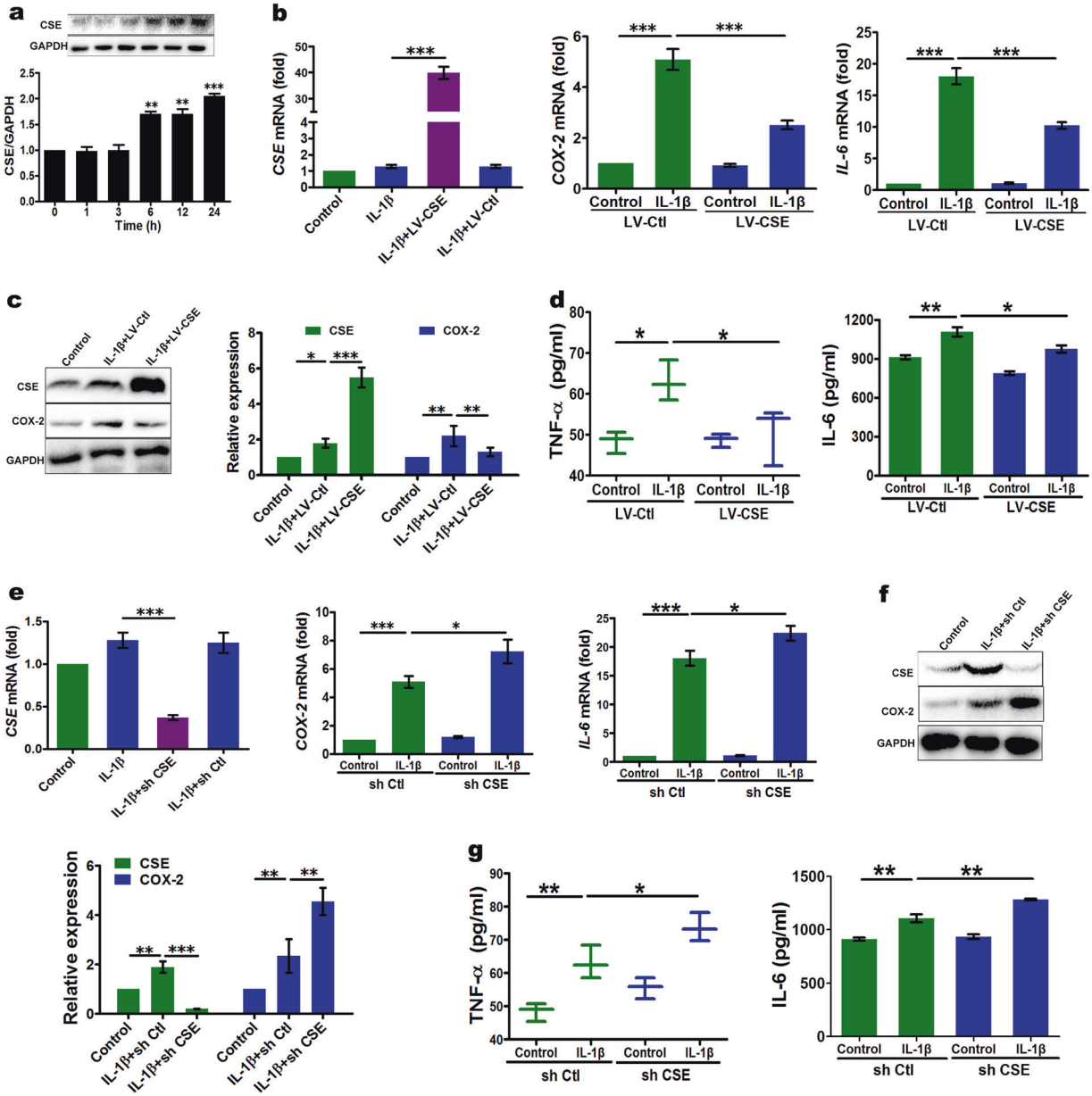

Fig. 1 CSE negatively regulates the IL-1β-induced inflammatory response in MH7A cells. **a** The expression level of CSE in MH7A, at the different times following IL-1β treatment, was determined by western blotting. **b**–**d** The overexpression of CSE resulted in decreased inflammatory mediators in MH7A cells. MH7A cells were infected with lentiviral cDNA-CSE (LV-CSE) or control empty vector (LV-Ctl) and were then stimulated with IL-1β (10 ng/ml). The mRNA expression levels of CSE, COX-2 and IL-6 were measured by qRT-PCR after stimulation for 3 h (**b**); the protein expression levels of CSE and COX-2 were assessed by western blotting after stimulation for 24 h (**c**); TNF-α and IL-6 production, in the culture supernatants, was assessed by ELISA (**d**). **e**–**g** CSE silencing resulted in increased inflammatory mediators in the MH7A cells. The MH7A cells were transfected with CSE-shRNA (sh CSE) or control empty vector (sh Ctl) and were then stimulated with IL-1β (10 ng/ml). The mRNA expression levels of CSE, COX-2 and IL-6 were measured by qRT-PCR after stimulation for 3 h (**e**); the protein expression levels of CSE and COX-2 were assessed by western blotting after stimulation for 24 h (**f**); TNF-α and IL-6 production, in the culture supernatants, was assessed by ELISA (**g**). All data were shown as the mean ± SEM from three independent experiments; *$p < 0.05$, **$p < 0.01$, ***$p < 0.001$

downregulation of IL-1β-induced TLR2 expression, following the knockdown of JMJD3, was also apparent by immunofluorescence (Fig. 2e).

We further investigated the level of H3K27me3 in the promoter of *TLR2* with a ChIP assay. Enrichment of H3K27me3 was observed in the promoter of *TLR2* in unstimulated control cells. However, we detected decreased H3K27me3 in the MH7A cells subjected to the IL-1β treatment. As expected, JMJD3 depletion reversed the decrease of H3K27me3 in the promoter of *TLR2* after the IL-1β treatment (Fig. 2f). Collectively, our findings suggested that JMJD3 was directly involved in *TLR2* gene activation by the demethylation of H3K27me3 on the promoter upon IL-1β treatment.

CSE inhibits the inflammatory response by mediating JMJD3 in IL-1β-stimulated MH7A cells

Next, we explored a functional link between CSE and JMJD3 in IL-1β-stimulated MH7A cells. As shown in Fig. 3a, b, the overexpression of CSE markedly downregulated the IL-1β-induced JMJD3 mRNA and protein levels. In contrast, CSE silencing resulted

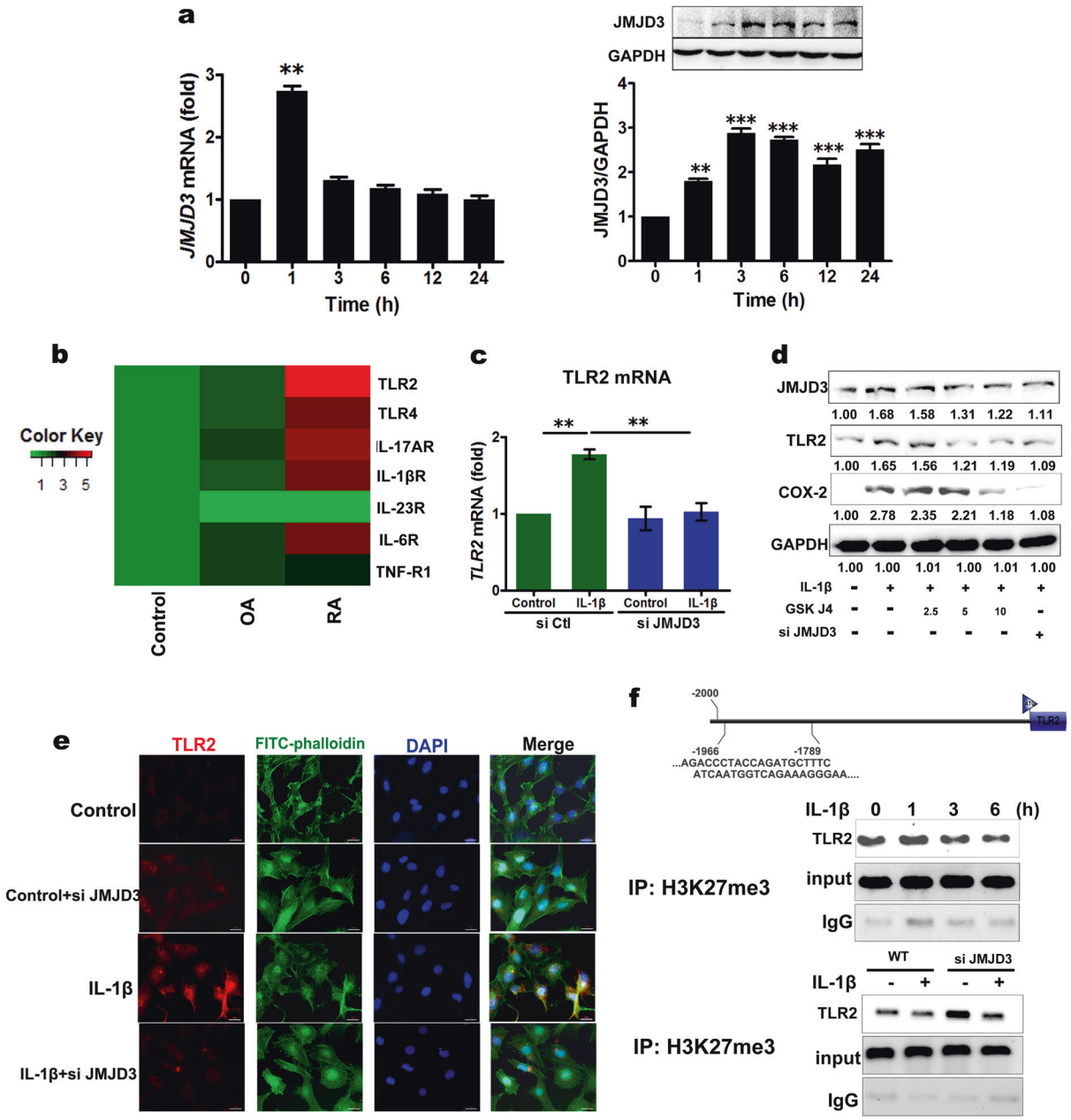

Fig. 2 The depletion of JMJD3 increases H3K27me3 in the *TLR2* promoter region and inhibits the IL-1β-induced inflammatory response in MH7A cells. **a** The expression level of JMJD3 in MH7A cells, at the different times following IL-1β treatment, was determined by qRT-PCR and western blotting. **b** The heatmap displays the relative abundances of the dominant membrane receptors in human SFs from normal, OA and RA patients. The green and red represent the minimum and the maximum relative abundance, respectively. The heatmap was made with R version 2.11.0 using the heatmap function. Control normal human, RA rheumatoid arthritis, OA osteoarthritis. **c** Decreased TLR2 expression in the JMJD3-downregulated cells. The MH7A cells were infected with control siRNA (si Ctl) or JMJD3 siRNA (si JMJD3) and were then stimulated with IL-1β (10 ng/ml). The mRNA expression of TLR2 was measured by qRT-PCR after stimulation for 3 h. **d**, **e** Inhibition of JMJD3 mitigated the IL-1β-induced inflammatory response in the MH7A cells. The MH7A cells were transfected with control or JMJD3 siRNA or treated with the indicated concentrations of GSK-J4 (JMJD3 inhibitor) and were then stimulated with IL-1β for 24 h. Western blot analysis of JMJD3, TLR2, COX-2 and GAPDH expression (**d**). MH7A cells were immunostained with an antibody against TLR2 (magnification, 200×) (**e**). **f** ChIP analysis for the H3K27me3 level in the TLR2 promoter region in the IL-1β-induced MH7A cells. H3K27me3 level in the IL-1β-induced MH7A cells for the indicated time. The MH7A cells were transfected with si Ctl or si JMJD3 and were then treated with IL-1β (10 ng/ml) for 6 h. The H3K27me3 level in the TLR2 promoter region. All of the data are shown as the mean ± SEM from three independent experiments; $^{**}p < 0.01$, $^{***}p < 0.001$

in markedly increased JMJD3 mRNA and protein levels (Fig. 3c, d). IL-1β-induced JMJD3 expression was downregulated by CSE, which was also determined by immunofluorescence (Fig. 3e). Taken together, these findings strongly suggested that CSE regulated the inflammatory response in IL-1β-stimulated MH7A cells, at least partially, through JMJD3 expression.

CSE regulates JMJD3 expression by the transcription factor Sp-1

We inspected the JMJD3 gene (*KDM6B*) promoter sequence 2000-bp nucleotides prior to the transcription start site with the aid of the online software ALGGEN (http://alggen.lsi.upc.es/). We identified a specific binding site for the transcription factor Sp-1, which provoked us to inquire whether CSE downregulated JMJD3 expression by reducing the

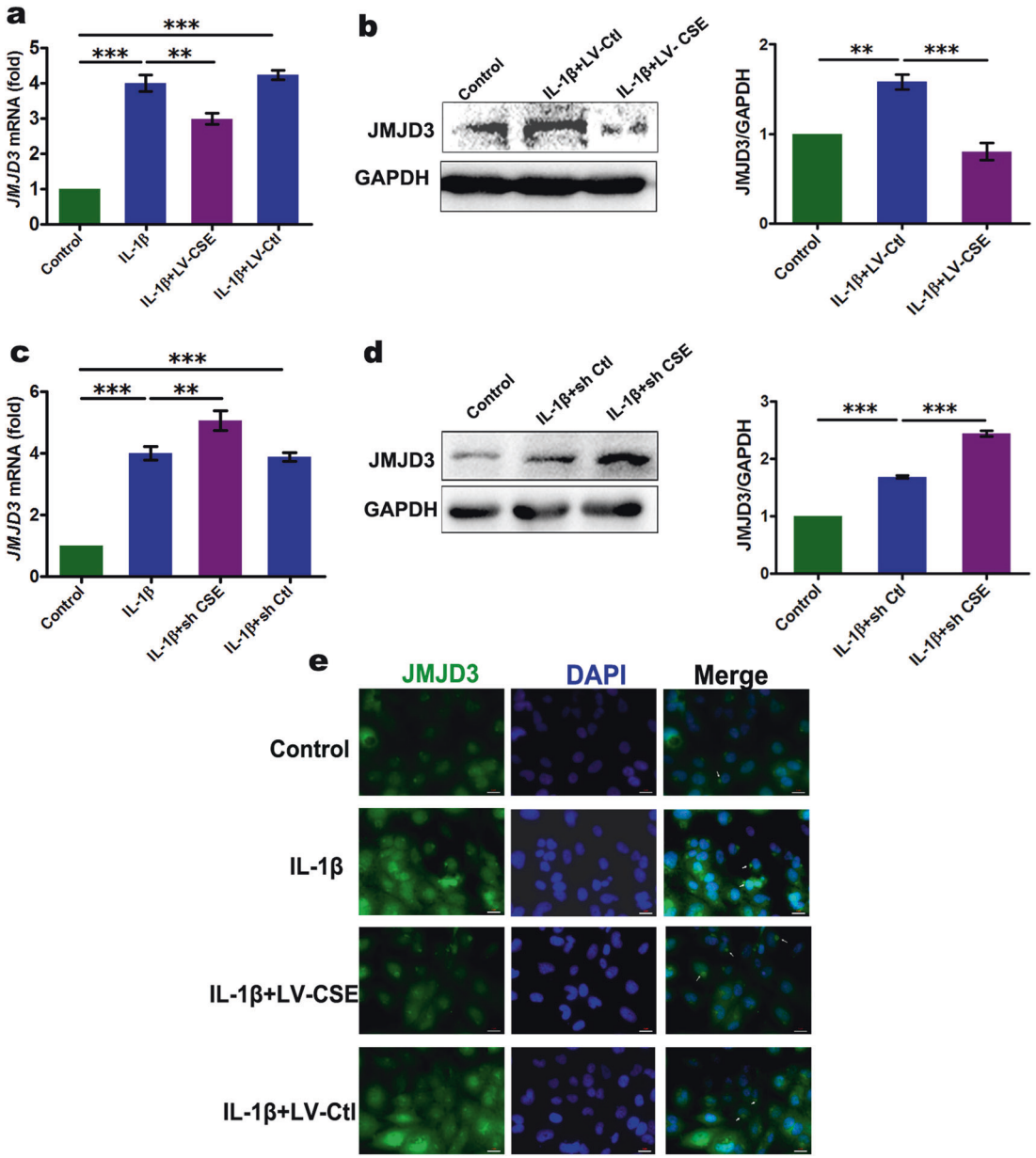

Fig. 3 CSE suppresses JMJD3 expression in IL-1β-induced MH7A cells. The MH7A cells were infected with lentiviral cDNA-CSE (LV-CSE) or control empty vector (LV-Ctl), and the cells were stimulated with IL-1β. The mRNA expression level of JMJD3 was measured by qRT-PCR after stimulation for 3 h (**a**). The protein expression level of JMJD3 was assessed by western blotting after stimulation for 24 h (**b**). The MH7A cells were transfected with CSE-shRNA (sh CSE) or control empty vector (sh Ctl), and the cells were stimulated with IL-1β. The mRNA expression level of JMJD3 was measured by qRT-PCR after stimulation for 3 h (**c**). The protein expression level of JMJD3 was assessed by western blotting after stimulation for 24 h (**d**). The MH7A cells were immunostained with an antibody against JMJD3 followed by FITC-labeled secondary antibodies and was mounted with fluorescence mounting medium with DAPI (magnification, 200×) (**e**). All of the data are shown as the mean ± SEM from three independent experiments; $^{**}p < 0.01$, $^{***}p < 0.001$

phosphorylation state of Sp-1. As illustrated in Fig. 4a, IL-1β stimulation elicited the phosphorylation of mitogen-activated protein kinase (MAPK; c-Jun N-terminal kinase 1/2 (JNK1/2), p38 and extracellular signal-regulated kinase 1/2 (ERK1/2)) and Sp-1. Furthermore, the overexpression of CSE significantly inhibited p38, ERK1/2 and Sp-1 activation, while in contrast, CSE knockdown induced the phosphorylation of ERK, p38 and Sp-1 (Fig. 4b). In addition, IL-1β-induced Sp-1 activation was suppressed by BIRB769 (p38 inhibitor, 400 nM) and U0126 (ERK inhibitor, 10 μM) (Fig. 4c). These data suggest that the MAPK and Sp-1 pathways were involved in CSE-mediated inflammation in IL-1β-stimulated MH7A cells. Furthermore, we noted that mithramycin (an Sp-1 inhibitor) inhibited JMJD3 expression in a concentration-dependent manner, with a concomitantly decreased production of IL-6 and COX-2 (Fig. 4d). As expected, the knockdown of Sp-1 also inhibited JMJD3 and COX-2 expression (Fig. 4e).

To confirm the direct binding of Sp-1 to the promoter of *KDM6B*, the cells were subjected to ChIP-PCR using primers flanking the core promoter regions of *KDM6B*. In the MH7A cells, ChIP-MYC resulted in an enrichment at the promoter of *KDM6B* (Fig. 4f). Furthermore, we determined the binding capacity of Sp-1 to its candidate sites by EMSA. When a biotin probe on the promoter region of *KDM6B* was subjected to EMSA, the results showed a shift complex with the MH7A cell nuclear extract. A competition assay was performed by preincubating the nuclear proteins from

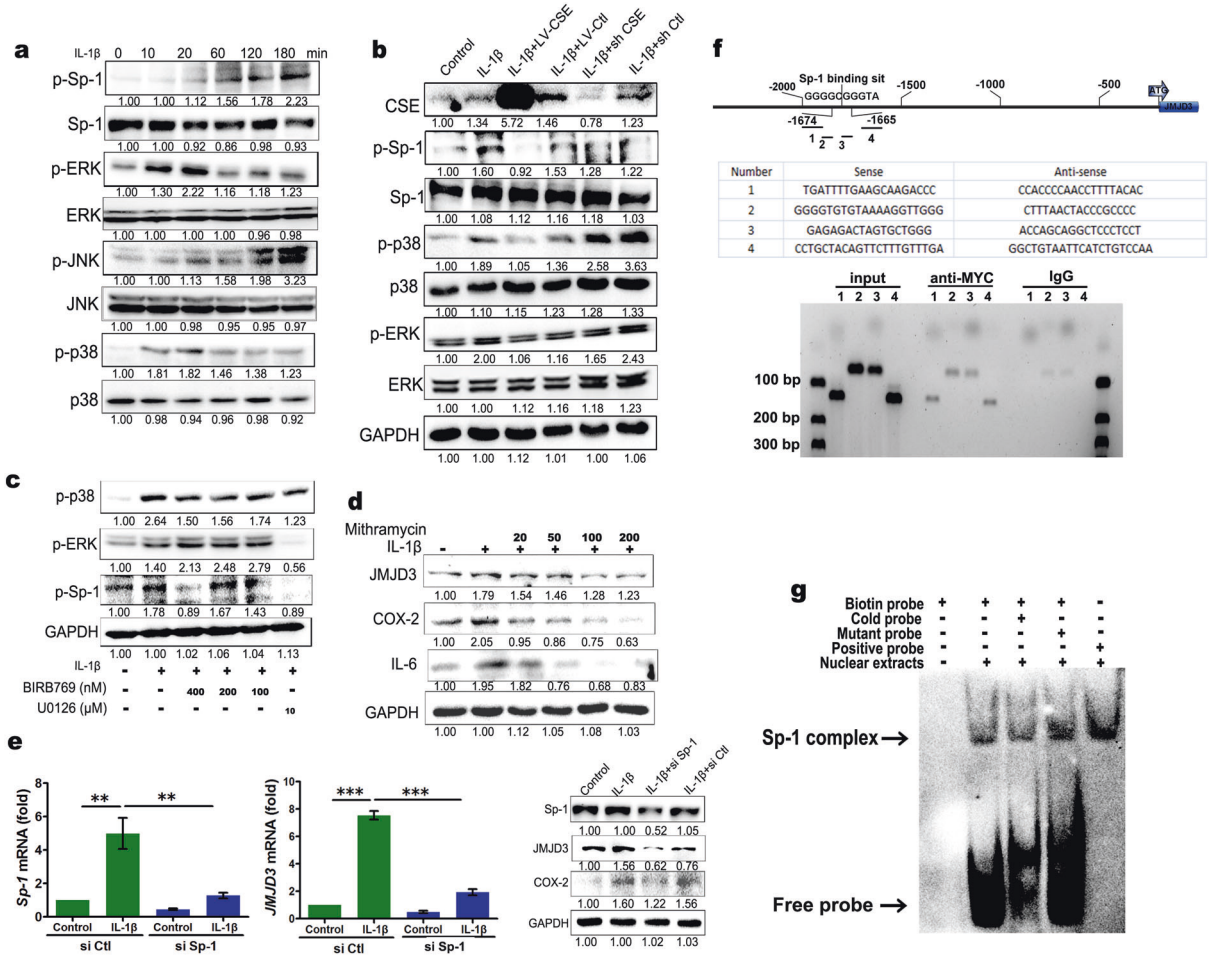

Fig. 4 CSE downregulates JMJD3 expression by inhibiting Sp-1 activation in IL-1β-induced MH7A cells. **a** IL-1β induced MAPK and Sp-1 signaling activation in the MH7A cells. **b** CSE negatively regulated Sp-1 activation. **c** The inhibition of ERK or p38 mitigated the Sp-1 activation. The MH7A cells were pretreated with the indicated concentrations of BIRB769 (ERK inhibitor) and U0126 (p38 inhibitor, 10 μM) for 1 h, and the cells were stimulated with IL-1β for 30 min. The cell lysates were prepared and blotted with phosphor-specific antibodies to Sp-1, ERK1/2 and p38 MAPK. **d** The Sp-1 inhibitor mithramycin suppressed JMJD3, COX-2 and IL-6 expression in the IL-1β-induced MH7A cells. **e** Silencing Sp-1 resulted in the decreased mRNA or protein expression of JMJD3 and COX-2 in the IL-1β-induced MH7A cells. **f** The MH7A cells were transfected with MYC-Sp-1, and different regions around the Sp-1 binding site were analyzed by ChIP and PCR using the MYC antibody. **g** Sp-1 bound to the *KDM6B* promoter was measured by EMSA. The ability of the MH7A cell nuclear extract to retard the shift of the Sp-1-binding oligos is shown. Arrows: Sp-1 shift, and free probe. All of the values are standardized with the untreated cell. All of the data are shown as the mean ± SEM from three independent experiments; $^{**}p < 0.01$, $^{***}p < 0.001$

the MH7A cells with a 20-fold molar excess of the unlabeled probe before the addition of the labeled probe (Fig. 4g). In addition, we used Firefly luciferase activity to further determine the effect of Sp-1 on human JMJD3 gene promoter activity (Fig. S2). These results suggested that Sp-1 bound to the promoter sequences of *KDM6B* to regulate its transcription.

CSE and JMJD3 regulate osteoclastogenesis and MH7A cell migration

A role for JMJD3 in murine osteoclast differentiation was suggested previously.[27,28] We further assessed the role played by JMJD3 and CSE in osteoclast differentiation and found that GSK-J4 (1 μM) significantly downregulated the number of $TRAP^+$ multinuclear cells (Fig. 5a). Conversely, PAG (an inhibitor of CSE) almost doubled the number of TRAP-positive osteoclasts (Fig. 5a), suggesting that CSE negatively regulated osteoclastogenesis in BMMs. To assess the potential cytotoxicity of PAG and GSK-J4, cell viability was evaluated using the CCK-8 assay. Neither PAG (0.5–2 mM) nor GSK-J4 (1 μM) affected cell viability. PAG was cytotoxic at concentrations of >4 mM (Fig. 5b). Taken together, these results suggested that PAG and GSK-J4 mediated osteoclast differentiation that was unrelated to cytotoxicity.

We further examined whether the increased expression of CSE and JMJD3 played a role in SF migration and invasion. The knockdown of CSE significantly increased the migrated numbers in the IL-1β-stimulated MH7A cells. In contrast, the number of migrated JMJD3 siRNA MH7A cells was significantly reduced (Fig. 5c). Taken together, our results suggested that CSE and JMJD3 exhibited the opposite effect on cell migration.

Exacerbation of arthritis in $CSE^{-/-}$ mice

Next, we used WT and $CSE^{-/-}$ mice to evaluate the severity of arthritis after CIA. As shown in Fig. 5d, safranin-O and toluidine blue staining indicated more severe aggravation of articular cartilage within the knee joints of the $CSE^{-/-}$ mice compared with the WT mice. Micro-CT imaging demonstrated a greater extent of bone destruction in the $CSE^{-/-}$ mice (Fig. 5e). Additionally, significant bone loss was seen in the WT mice compared with the vehicle controls, but the $CSE^{-/-}$ mice significantly aggravated this loss, as indicated by the decreased BMD (Fig. 5f).

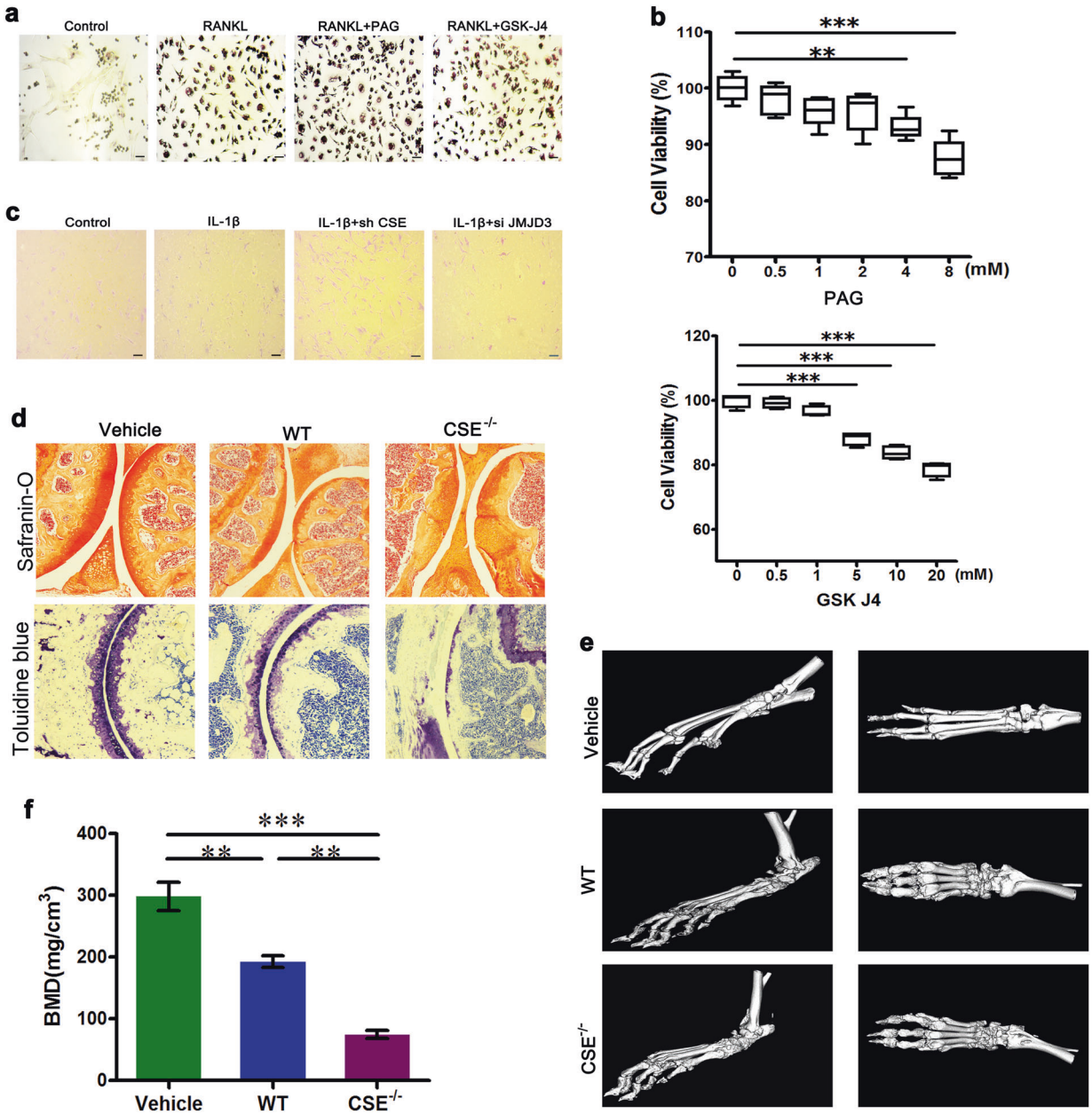

Fig. 5 Knockout of CSE exacerbates bone erosion in collagen-induced arthritis (CIA) mice. **a** PAG and GSK-J4 regulated RANKL-induced osteoclast formation from BMMs. BMMs were cultured with M-CSF (30 ng/ml) and RANKL (50 ng/ml) in the presence of 2 mM PAG (CSE inhibitor) or 1 μM GSK-J4 (JMJD3 inhibitor) for 4 days. The cells were fixed, and TRAP staining was performed. Scale bar, 50 μm. **b** BMMs were treated with the indicated concentrations of PAG or GSK-J4 for 48 h. Cell viability was measured by a CCK8 assay. All of the values were standardized with the untreated cell. **c** Silencing CSE or JMJD3 regulated IL-1β-induced MH7A migration. Silencing CSE expression in MH7A cells significantly increased the migration ability of these cells through the transwell; conversely, JMJD3 knockdown significantly reduced the migration ability of these cells. Scale bar, 50 μm. **d** Sections of articular tissue from Vehicle, WT and $CSE^{-/-}$ mice with CIA were stained with safranin O and toluidine blue. **e** Representative CT scan photographs of the hind paws from the vehicle, WT and $CSE^{-/-}$ mice with CIA at day 30 after the second immunization. Scale bar, 100 μm. **f** The cortical bone mineral density in the femur and tibia were calculated. BMD bone mineral density. All of the data are shown as the mean ± SEM; $n = 6$, $^{**}p < 0.01$, $^{***}p < 0.001$

Interestingly, the $CSE^{-/-}$ mice developed a more severe form of arthritis, as seen by the significant increases in soft tissue swelling and the mean arthritic score (Fig. 6a, b). The increased severity of arthritis in the $CSE^{-/-}$ mice was also associated with an augmented infiltration of immune cells and pannus formation in the affected joints (Fig. 6c). Additionally, the spleen weight of the $CSE^{-/-}$ mice was significantly increased in comparison to the WT group (Fig. 6d). Furthermore, the level of serum inflammation mediators in the $CSE^{-/-}$ mice with CIA also increased compared with the WT mice (Fig. 6e). Overall, these data indicate that CSE is an important modifier of arthritis, delaying key pathological metrics of disease, including the cartilage degradation and bone erosion. Furthermore, the expression of JMJD3 and TLR2 was substantially increased in the $CSE^{-/-}$ mice compared with the WT mice (Fig. 6f), suggesting that CSE knockout promoted inflammation by increasing JMJD3 expression in the CIA mice. In our latest study, we found that JMJD3 regulates the proliferation of SFs and joint destruction in RA28 and that the blockade of JMJD3 activity affected the development of CIA in mice. The incidence of arthritis and joint swelling in the GSK-J4-treated

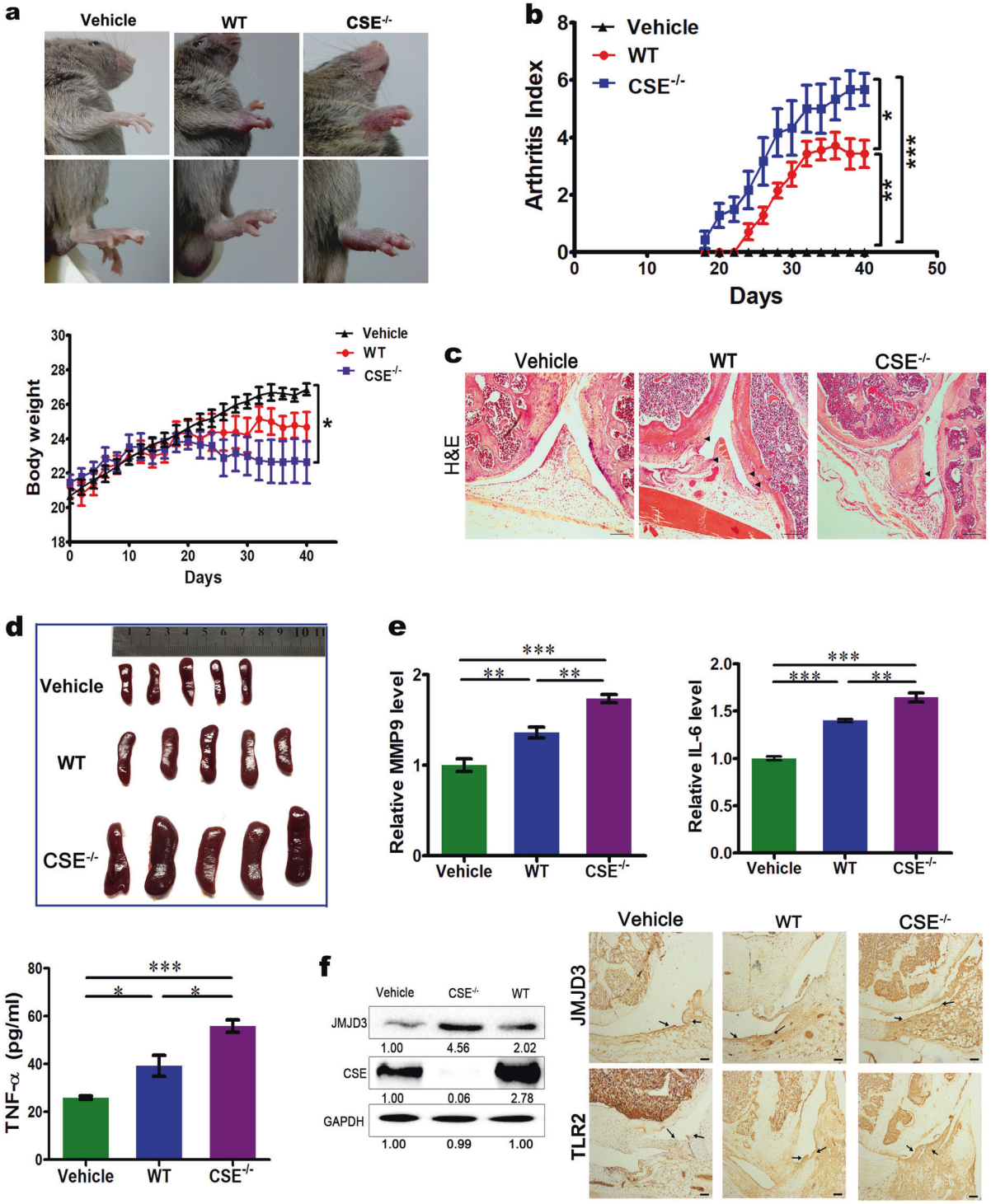

Fig. 6 Knockout of CSE exacerbates collagen-induced arthritis (CIA) development. **a** Macroscopic evidence of arthritis, such as erythema or swelling, was markedly observed in the WT mice, while the arthritis severity was significantly exacerbated in the $CSE^{-/-}$ mice. **b** The body weight changes and arthritis severity scores in the CIA mice were recorded daily after the second immunization. ($n = 7$). **c** H&E staining analysis of representative knee sections from the vehicle, WT and $CSE^{-/-}$ mice with CIA at day 30 after the second immunization. **d** Gross spleen morphology from the vehicle, WT and $CSE^{-/-}$ mice with CIA. **e** The MMP9, IL-6 and TNF-α levels in the serum of the vehicle, WT and $CSE^{-/-}$ mice with CIA, at day 30 after the second immunization were measured by ELISA. **f** The JMJD3 and CSE protein levels in the synovial tissues were detected by western blotting, and TLR2 and JMJD3 expression in the synovium samples was assayed by immunohistochemical detection in the vehicle, WT and $CSE^{-/-}$ mice with CIA. All data are shown as the mean ± SEM, $n = 7$, $^{*}p < 0.05$, $^{**}p < 0.01$, $^{***}p < 0.001$

mice was significantly less than that in the CIA mice (Fig. S3a). The H&E and toluidine blue staining also indicated that GSK-J4 treatment suppressed the accumulation of inflammatory cells in the joint space and the pathological changes (Fig. S3b). In addition, GSK-J4 treatment caused a dramatic decrease in the levels of TNF-α (Fig. S3c). Thus, these data further determined the inhibitory effect of GSK-J4 on cartilage destruction and inflammation in joints.

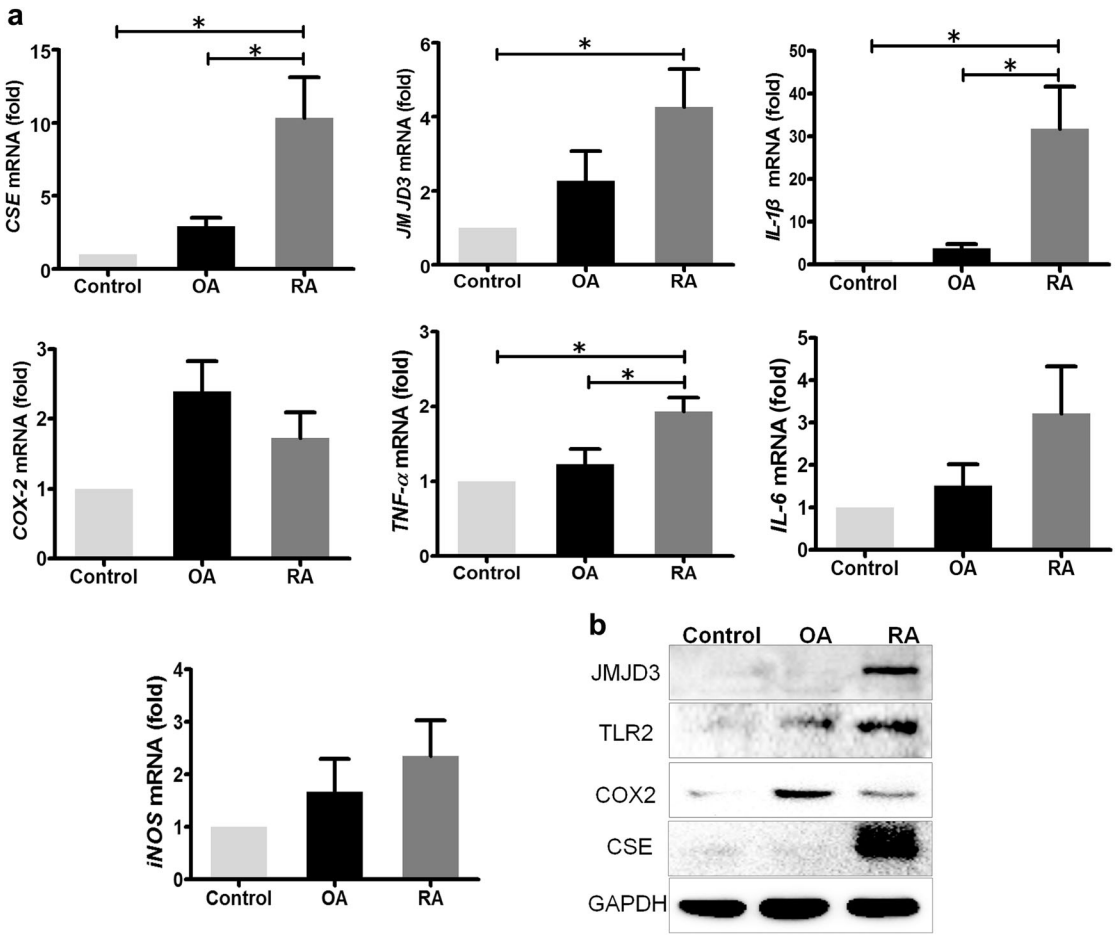

Fig. 7 JMJD3 and CSE are upregulated in the SFs from the RA patients. **a** qRT-PCR analysis of JMJD3, CSE and the inflammatory mediator levels in the SFs from control human, OA and RA patients. **b** Western blotting analysis of JMJD3, CSE and the inflammatory mediators in the SFs from control human, OA and RA patients. Control normal human, RA rheumatoid arthritis, OA osteoarthritis. All of the data are shown as the mean ± SEM from three independent experiments; *$p < 0.05$

Evidence of JMJD3 and CSE upregulation in human RA SFs

The expression of JMJD3 and CSE in the SFs from RA patients was assessed. CSE and JMJD3 mRNA levels in RA SFs were significantly increased compared to healthy or OA samples. The expression of the inflammatory mediators and TLR2 was also consistently increased (Fig. 7a). Furthermore, JMJD3 and CSE protein expression was significantly higher in the SFs of the RA patients compared with the OA patients and healthy subjects (Fig. 7b). These data further raised the possibility that increased JMJD3 and CSE expression may be implicated in the pathogenesis of RA.

DISCUSSION

In this study, we provide evidence suggesting that the anti-inflammatory effect of endogenous CSE/H_2S is mediated, at least in part, by the histone demethylase JMJD3. Thus, initially, we observed upregulated expression of both CSE and JMJD3 in the IL-1β-induced MH7A cells and in the joints of the arthritic mice as well as in human RA samples. Furthermore, we identified an anti-inflammatory effect of CSE that occurs via the regulation of the JMJD3-dependent gene expression network in RA. Importantly, we also showed, for the first time, that CSE ameliorated the histone demethylase JMJD3-mediated autoimmune response by the transcription factor Sp-1. Meanwhile, JMJD3 regulated inflammation, at least partially, by changing H3K27me3 levels in the membrane receptor *TLR2* promoter, which subsequently led to transcriptional upregulation (see working model in Fig. 8). Thus, this knowledge is highly relevant to a better understanding of the mechanisms of RA and defines the potential novel anti-inflammatory effects of CSE/H_2S therapy.

The pathogenesis of RA is intricate and includes various immune cell populations, including T cells, B cells, macrophages and SFs.[29–31] The formation of invasive pannus, a thickened layer of synovial tissue that erodes cartilage and bone, is the pathological hallmark of RA.[29] SFs play an important role in the pathogenesis of RA by synthesizing cytokines and chemokines, which are involved in the process of joint tissue damage in RA.[30,32] Thus, therapeutic strategies that block the actions of RA-SF-dependent effector molecules need to be investigated. H_2S is also involved in inflammation, and its role has been debated for many years.[33,34] However, recent evidence indicates that H_2S is primarily anti-inflammatory.[14,35] In accordance with previous observations, the data presented in our study showed that endogenous CSE has anti-inflammatory properties in RA. The effect of CSE/H_2S on IL-1β-induced MH7A cells was confirmed by the downregulation of inflammatory mediators, such as TNF-α, COX-2 and IL-6, which are well-known downstream pro-inflammatory marker genes for RA.[36] In contrast, the knockdown of CSE, to decrease endogenous H_2S, augmented the inflammatory response in IL-1β-induced MH7A cells. Furthermore, the in vivo knockout of CSE in the CIA model mice dramatically increased the severity of arthritis. The pathological process of RA is often accompanied by bone destruction and severe joint deformities, eventually influencing movement function. In our present study, the $CSE^{-/-}$ mice developed severe joint

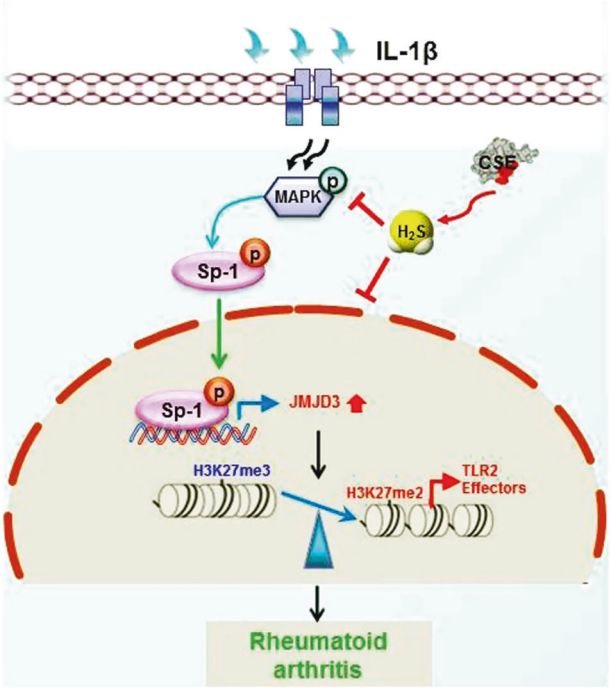

Fig. 8 Working model of the mechanism by which cystathionine-γ-lyase ameliorates the histone demethylase JMJD3-mediated autoimmune response in rheumatoid arthritis. Endogenous CSE/H_2S decreases the JMJD3 protein level by inhibiting the transcription factor Sp-1, leading to H3K27me3 marker enrichment in the promoter of the *TLR2* gene, which further ameliorates RA

inflammation with significant bone erosion, which was supported by the fact that the deletion of CSE increased osteoclastogenesis.

The precise sites and mechanisms of action of H_2S, as an inflammatory mediator, are not well established; however, existing data indicate many diverse targets.[19,37,38] Interestingly, many histone markers, including H3K27me3, are implicated in inflammation and disease pathogenesis.[39] It is well established that H3K27me3 brings about the silencing of genes, and JMJD3 is a known H3K27me3 demethylase.[40] On the other hand, very few studies are available that address the role of endogenous CSE in histone methylation modification. In the present work, we provided evidence that JMJD3 was critically important for the anti-inflammatory effect of CSE in RA, which was the first demonstration, to our knowledge, that such an epigenetic mechanism could contribute to CSE/H_2S signaling. Sp-1, a member of the family of Sp/Krüppel-like factors, is a well-characterized transcription factor involved in the basal regulation of a number of genes.[41] Interestingly, our present results revealed that the overexpression of CSE in MH7A cells led to decreased levels of phosphorylated Sp-1 and inhibited JMJD3 expression. Importantly, we demonstrated, for the first time, that the knockdown of Sp-1 or the use of the specific inhibitor, mithramycin, attenuated JMJD3 expression in IL-1β-induced MH7A cells. Furthermore, we determined that Sp-1 bound to the promoter of the KDM6B gene and showed that JMJD3 expression was controlled by Sp-1. These findings provided the first evidence that CSE/H2S potentially controlled JMJD3 expression via the transcription factor Sp-1.

The TLR family of proteins are immune receptor proteins expressed on immune cells and SFs.[42] Thus, the presence of TLR2 in synovial tissue and in the macrophages of patients with clinically active disease contributes to symptom severity via the production of inflammatory cytokines. More importantly, we screened a series of membrane receptors by a heatmap analysis using the SFs from normal human, OA and RA patients and expected to find causal relationships between RA and membrane receptors. We found that the mRNA level of TLR2 was the most significant increase among the indicated three groups. Meanwhile, it is reported that downregulating TLR2 alleviates inflammation in a mouse arthritis model.[43] These results suggest that the regulation of TLR2 expression in SFs is of great significance for RA treatment. Interestingly, other reports show that JMJD3 is implicated in regulating TLR responses.[44,45] In this study, we found that JMJD3 was upregulated in the IL-1β-induced SFs, enhancing H3K27me3 demethylase activity and thus reducing the H3K27me3 repressive mark on the *TLR2* promoter, which may therefore improve the expression of TLR2 and inflammation-related genes. In contrast, the JMJD3 inhibitor GSK-J4 or JMJD3 silencing decreased TLR2 expression by maintaining the repressive marker H3K27me3 on the promoter. We showed that JMJD3 regulated the inflammatory response by controlling the methylation status of H3K27me3 on the promoters of target genes. This was in agreement with a recent study showing that a JMJD3 inhibitor significantly reduced the inflammatory reaction in mice with CIA arthritis.

In conclusion, upregulated CSE and JMJD3 were found in the SFs of RA patients and in the joints of arthritis mice. Moreover, CSE negatively regulated the inflammatory response in SFs and prevented the progression of CIA, which was mainly attributed to inhibiting JMJD3 in RA. CSE negatively regulated JMJD3 expression mainly by mediating the Sp-1 pathway. Our data provided a novel insight into the molecular mechanism of endogenous CSE/H_2S regulating the inflammatory response in RA pathogenesis, suggesting that H_2S may become a potential therapeutic approach for RA.

ACKNOWLEDGEMENTS

This work was supported by grants from National Natural Science Foundation of China (No. 81673428; 81330080), a key laboratory program of the Education Commission of Shanghai Municipality (No. ZDSYS14005).

ADDITIONAL INFORMATION

The online version of this article (https://doi.org/10.1038/s41423-018-0037-8) contains supplementary material.

Competing interests: The authors declare no competing interests.

REFERENCES

1. Walsh, D. A. & McWilliams, D. F. Mechanisms, impact and management of pain in rheumatoid arthritis. *Nat. Rev. Rheumatol.* **10**, 581–592 (2014).
2. Anderson, K. O., Bradley, L. A., Young, L. D., McDaniel, L. K. & Wise, C. M. Rheumatoid arthritis: review of psychological factors related to etiology, effects, and treatment. *Psychol. Bull.* **98**, 358–387 (1985).
3. Choy, E. H. & Panayi, G. S. Cytokine pathways and joint inflammation in rheumatoid arthritis. *N. Engl. J. Med.* **344**, 907–916 (2001).
4. Wang L. et al. TXNDC5 synergizes with HSC70 to exacerbate the inflammatory phenotype of synovial fibroblasts in rheumatoid arthritis through NF-kappaB signaling. *Cell Mol Immunol.* **4**, 1–12 (2017).
5. Smolen, J. S. et al. EULAR recommendations for the management of rheumatoid arthritis with synthetic and biological disease-modifying antirheumatic drugs: 2013 update. *Ann. Rheum. Dis.* **73**, 492–509 (2014).
6. Zhou, H. F. et al. Peptide-siRNA nanocomplexes targeting NF-kappaB subunit p65 suppress nascent experimental arthritis. *J. Clin. Invest.* **124**, 4363–4374 (2014).
7. Salliot, C. et al. Infections during tumour necrosis factor-alpha blocker therapy for rheumatic diseases in daily practice: a systematic retrospective study of 709 patients. *Rheumatol. (Oxf.)* **46**, 327–334 (2007).
8. Emery, P. et al. IL-6 receptor inhibition with tocilizumab improves treatment outcomes in patients with rheumatoid arthritis refractory to anti-tumour necrosis factor biologicals: results from a 24-week multicentre randomised placebo-controlled trial. *Ann. Rheum. Dis.* **67**, 1516–1523 (2008).
9. Medzhitov, R. & Horng, T. Transcriptional control of the inflammatory response. *Nat. Rev. Immunol.* **9**, 692–703 (2009).

10. Han, X. et al. Epigenetic regulation of tumor necrosis factor alpha (TNFalpha) release in human macrophages by HIV-1 single-stranded RNA (ssRNA) is dependent on TLR8 signaling. *J. Biol. Chem.* **287**, 13778–13786 (2012).
11. Das, N. D. et al. Gene networking and inflammatory pathway analysis in a JMJD3 knockdown human monocytic cell line. *Cell Biochem. Funct.* **30**, 224–232 (2012).
12. Cao, R. et al. Role of histone H3 lysine 27 methylation in Polycomb-group silencing. *Science* **298**, 1039–1043 (2002).
13. Ekundi-Valentim, E. et al. Differing effects of exogenous and endogenous hydrogen sulphide in carrageenan-induced knee joint synovitis in the rat. *Br. J. Pharmacol.* **159**, 1463–1474 (2010).
14. Wallace, J. L. & Wang, R. Hydrogen sulfide-based therapeutics: exploiting a unique but ubiquitous gasotransmitter. *Nat. Rev. Drug. Discov.* **14**, 329–345 (2015).
15. Stipanuk, M. H. & Beck, P. W. Characterization of the enzymic capacity for cysteine desulphhydration in liver and kidney of the rat. *Biochem. J.* **206**, 267–277 (1982).
16. Awata, S., Nakayama, K., Suzuki, I., Sugahara, K. & Kodama, H. Changes in cystathionine gamma-lyase in various regions of rat brain during development. *Biochem. Mol. Biol. Int.* **35**, 1331–1338 (1995).
17. Zanardo, R. C. et al. Hydrogen sulfide is an endogenous modulator of leukocyte-mediated inflammation. *FASEB J.* **20**, 2118–2120 (2006).
18. Cunha, T. M. et al. Dual role of hydrogen sulfide in mechanical inflammatory hypernociception. *Eur. J. Pharmacol.* **590**, 127–135 (2008).
19. Oh, G. S. et al. Hydrogen sulfide inhibits nitric oxide production and nuclear factor-kappaB via heme oxygenase-1 expression in RAW264.7 macrophages stimulated with lipopolysaccharide. *Free Radic. Biol. Med.* **41**, 106–119 (2006).
20. Wu, W. J. et al. S-propargyl-cysteine attenuates inflammatory response in rheumatoid arthritis by modulating the Nrf2-ARE signaling pathway. *Redox Biol.* **10**, 157–167 (2016).
21. Impellizzeri, D. et al. Oleuropein aglycone, an olive oil compound, ameliorates development of arthritis caused by injection of collagen type II in mice. *J. Pharmacol. Exp. Ther.* **339**, 859–869 (2011).
22. Neidhart, M., Gay, R. E. & Gay, S. Anti-interleukin-1 and anti-CD44 interventions producing significant inhibition of cartilage destruction in an in vitro model of cartilage invasion by rheumatoid arthritis synovial fibroblasts. *Arthritis Rheum.* **43**, 1719–1728 (2000).
23. Mazess, R. B., Nord, R., Hanson, J. A. & Barden, H. S. Bilateral measurement of femoral bone mineral density. *J. Clin. Densitom.* **3**, 133–140 (2000).
24. Kawai, M. et al. A circadian-regulated gene, Nocturnin, promotes adipogenesis by stimulating PPAR-gamma nuclear translocation. *Proc. Natl. Acad. Sci. USA* **107**, 10508–10513 (2010).
25. Mukaida, N., Mahe, Y. & Matsushima, K. Cooperative interaction of nuclear factor-kappa B- and cis-regulatory enhancer binding protein-like factor binding elements in activating the interleukin-8 gene by pro-inflammatory cytokines. *J. Biol. Chem.* **265**, 21128–21133 (1990).
26. Hashizume, R. et al. Pharmacologic inhibition of histone demethylation as a therapy for pediatric brainstem glioma. *Nat. Med.* **20**, 1394–1396 (2014).
27. Yasui, T. et al. Epigenetic regulation of osteoclast differentiation: possible involvement of Jmjd3 in the histone demethylation of Nfatc1. *J. Bone Miner. Res.* **26**, 2665–2671 (2011).
28. Jia W. et al. Histone demethylase JMJD3 regulates fibroblast-like synoviocyte-mediated proliferation and joint destruction in rheumatoid arthritis. *FASEB J.* 2018; fj201701483R.
29. McInnes, I. B. & Schett, G. The pathogenesis of rheumatoid arthritis. *N. Engl. J. Med.* **365**, 2205–2219 (2011).
30. Bartok, B. & Firestein, G. S. Fibroblast-like synoviocytes: key effector cells in rheumatoid arthritis. *Immunol. Rev.* **233**, 233–255 (2010).
31. Guo N. et al. A critical epitope in CD147 facilitates memory CD4(+) T-cell hyperactivation in rheumatoid arthritis. *Cell Mol. Immunol.* 2018; in press. https://doi.org/10.1038/s41423-018-0012-4.
32. Leech, M. T. & Morand, E. F. Fibroblasts and synovial immunity. *Curr. Opin. Pharmacol.* **13**, 565–569 (2013).
33. Li, T. et al. Regulatory effects of hydrogen sulfide on IL-6, IL-8 and IL-10 levels in the plasma and pulmonary tissue of rats with acute lung injury. *Exp. Biol. Med. (Maywood).* **233**, 1081–1087 (2008).
34. Zhang, H. & Bhatia, M. Hydrogen sulfide: a novel mediator of leukocyte activation. *Immunopharmacol. Immunotoxicol.* **30**, 631–645 (2008).
35. Wallace, J. L., Caliendo, G., Santagada, V., Cirino, G. & Fiorucci, S. Gastrointestinal safety and anti-inflammatory effects of a hydrogen sulfide-releasing diclofenac derivative in the rat. *Gastroenterology* **132**, 261–271 (2007).
36. Choi, H. M. et al. Adiponectin may contribute to synovitis and joint destruction in rheumatoid arthritis by stimulating vascular endothelial growth factor, matrix metalloproteinase-1, and matrix metalloproteinase-13 expression in fibroblast-like synoviocytes more than proinflammatory mediators. *Arthritis Res. Ther.* **11**, R161 (2009).
37. Gong, Q. H. et al. Hydrogen sulfide attenuates lipopolysaccharide-induced cognitive impairment: a pro-inflammatory pathway in rats. *Pharmacol. Biochem. Behav.* **96**, 52–58 (2010).
38. Zhang, Q. et al. Hydrogen sulfide attenuates hypoxia-induced neurotoxicity through inhibiting microglial activation. *Pharmacol. Res.* **84**, 32–44 (2014).
39. Bayarsaihan, D. Epigenetic mechanisms in inflammation. *J. Dent. Res.* **90**, 9–17 (2011).
40. Swigut, T. & Wysocka, J. H3K27 demethylases, at long last. *Cell* **131**, 29–32 (2007).
41. Zhang, X., Li, L., Fourie, J., Davie, J. R. & Guarcello VDiasio, R. B. The role of Sp1 and Sp3 in the constitutive DPYD gene expression. *Biochim. Biophys. Acta* **1759**, 247–256 (2006).
42. Kawai, T. & Akira, S. The role of pattern-recognition receptors in innate immunity: update on Toll-like receptors. *Nat. Immunol.* **11**, 373–384 (2010).
43. Joosten, L. A. et al. Toll-like receptor 2 pathway drives streptococcal cell wall-induced joint inflammation: critical role of myeloid differentiation factor 88. *J. Immunol.* **171**, 6145–6153 (2003).
44. De Santa, F. et al. The histone H3 lysine-27 demethylase Jmjd3 links inflammation to inhibition of polycomb-mediated gene silencing. *Cell* **130**, 1083–1094 (2007).
45. Kruidenier, L. et al. A selective jumonji H3K27 demethylase inhibitor modulates the proinflammatory macrophage response. *Nature* **488**, 404–408 (2012).